

Long-Range Order in Thick, Unstrained $\text{Si}_{0.5}\text{Ge}_{0.5}$ Epitaxial Layers

F. K. LeGoues, V. P. Kesan, and S. S. Iyer

IBM Research Division, T. J. Watson Research Center, Yorktown Heights, New York 10598

(Received 10 October 1989)

We observe, for the first time, long-range order in thick, unstrained SiGe alloys, with and without boron doping. This ordering occurs along the four equivalent $\langle 111 \rangle$ directions. The ordered domains are randomly shaped, and correspond to alternating double layers of Si and Ge. Bond-energy arguments are used to explain the formation of this new phase.

PACS numbers: 61.55.Hg, 61.50.Ks

Order-disorder transitions have recently been observed in several semiconductor systems.¹⁻⁴ These phase transitions have potential technological applications, e.g., Suzuki and Gomyo⁵ demonstrated changes in the band gap of GaInP/GaAs due to ordering. They are also fascinating from a purely scientific point of view. Indeed, in the SiGe case, for example, it is generally believed that bulk alloys are model random solutions where long anneals over a wide temperature range fail to produce ordering.⁶ Still, ordering has been observed in SiGe strained-layer superlattices.^{2,3} This was tentatively explained by considering the stabilizing influence of strain upon a metastable, ordered SiGe phase.⁷⁻⁹ The conditions of growth, composition, and strain for which ordering can be expected still remain somewhat obscure, as exemplified by recent work on SiGe superlattices grown on Si(100), Si(110), and Si(111),¹⁰ where no ordering could be observed under the growth conditions. In this paper, we show, for the first time, that ordering can occur in thick, *essentially unstrained* $\text{Si}_{0.5}\text{Ge}_{0.5}$ layers.

The ordered alloy consists of alternating double layers of Si and Ge along the $\langle 111 \rangle$ direction. This results in what has been called⁷⁻⁹ a "microscopically strained" structure, i.e., not all bond lengths in the unit cell are expected to be equal to each other or to the ideal tetrahedral bond length. The formation of this microscopically strained phase is explained in terms of its lower chemical energy, which may counterbalance its higher mechanical energy. Ordering occurs as large domains distributed along all four $\langle 111 \rangle$ directions.

The samples used in this study were grown by conventional solid source molecular-beam epitaxy, between 390 and 475°C on Si(100) substrates. Figure 1 shows a cross section of the sample presented in detail here. It corresponds to a double-barrier resonant-tunneling device,¹¹ but, for the present purpose, only the top 5000-Å layer of $\text{Si}_{0.5}\text{Ge}_{0.5}$ is of interest. The underlying layers are only important in that they provide a relaxed substrate for the top layer. In order to rule out any effect due to the underlayers or the boron doping, a simpler

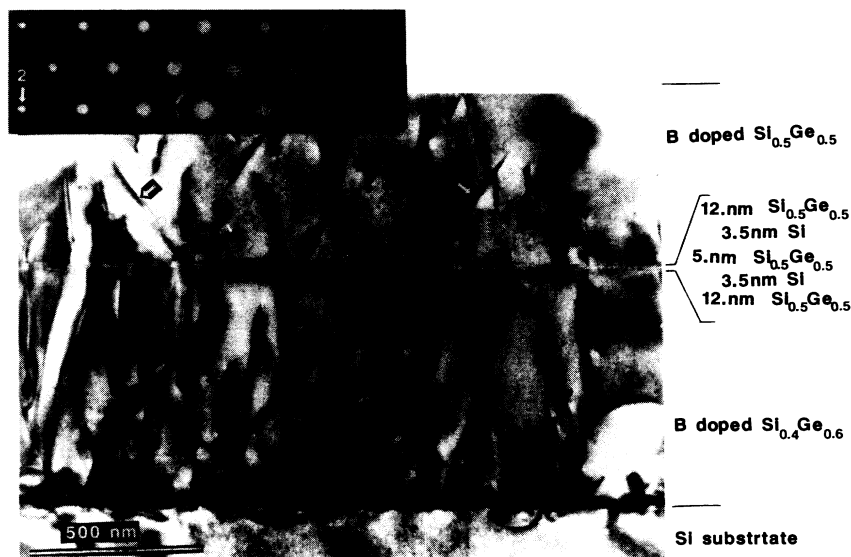


FIG. 1. Cross-sectional view and diffraction pattern of the samples. The arrows on the image show twins. In the diffraction pattern, the arrow marked 1 shows the extra spot due to ordering. The arrow marked 2 shows the splitting of the high-order spots due to the mismatch between substrate and layer.

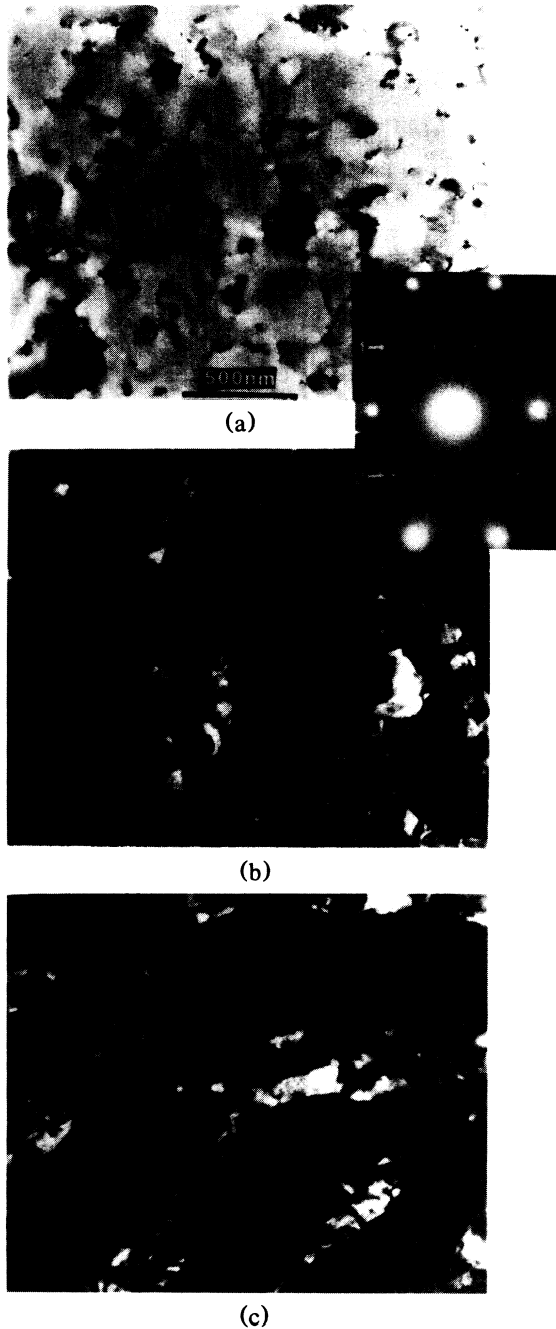


FIG. 2. (a) Bright field and diffraction pattern corresponding to the dark fields shown in (b) and (c). The zone axis is (013). (b) Dark field obtained using spot 1 on diffraction pattern. (c) Dark field obtained using spot 2 on diffraction pattern.

structure, consisting of 7500-Å undoped $\text{Si}_{0.5}\text{Ge}_{0.5}/\text{Si}(100)$ was also investigated.

As can be seen in Fig. 1, a large number of defects are present, accommodating the lattice-parameter difference between the epitaxial layer and the substrate. Note that although some of these defects are twins along the $\langle 111 \rangle$ directions¹⁰ (see arrows in figure), the majority of de-

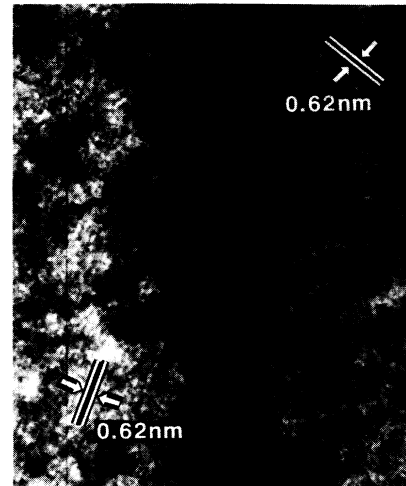


FIG. 3. High resolution of a domain boundary between two ordered zones with different orientations.

fects can be shown to be dislocations. The lattice-parameter difference is measured directly from the diffraction pattern and is found to be 0.02 ± 0.005 , as expected for a relaxed $\text{Si}_{0.5}\text{Ge}_{0.5}$ layer. The diffraction pattern also shows that superlattice reflections are present at $\frac{1}{2}\{111\}$, indicating ordering. Unlike the diffraction pattern presented by Ourmazd and Bean, no streaks are present, indicating that the ordered phase does not exhibit, in this case, a platelet morphology. Indeed, Fig. 2, which shows dark-field micrographs obtained for the (013) zone axis from a planar-view sample, demonstrates that the extra reflections present in this orientation arise from two differently oriented domains which are about half a micron wide and randomly shaped. Figure 3 shows a high-resolution image obtained for a (110) zone axis (in cross section) by choosing an objective aperture size just large enough to image the extra $\frac{1}{2}\{111\}$ reflections, corresponding to a lattice spacing of 6.2 Å, but not large enough to image the $\{111\}$ lattice spacing. This picture shows a domain boundary, where the ordering occurs along two different $\{111\}$ planes on each side of the boundary. Note that the quality of the image is poor due to the comparative weakness of the extra reflections. Figure 4(a) shows diffraction patterns obtained from a planar-view sample, for five different zone axes. Extra reflections are present in all of these pictures and are strong enough to be classified by their intensity: Note, for example, that, on the (013) zone axis, the $\frac{1}{2}\{133\}$ spot is significantly brighter than the $\frac{1}{2}\{113\}$ spot. Table I summarizes the spot intensities. By tilting around the (001) zone axis, in planar view, one can investigate all four $\langle 111 \rangle$ directions and thus convince oneself that all four variants exist. This can also be seen by comparing the diffraction patterns shown in Fig. 1 and Fig. 4: Since one of these is a planar view and the other is a cross section, three of the four $\langle 111 \rangle$ directions are

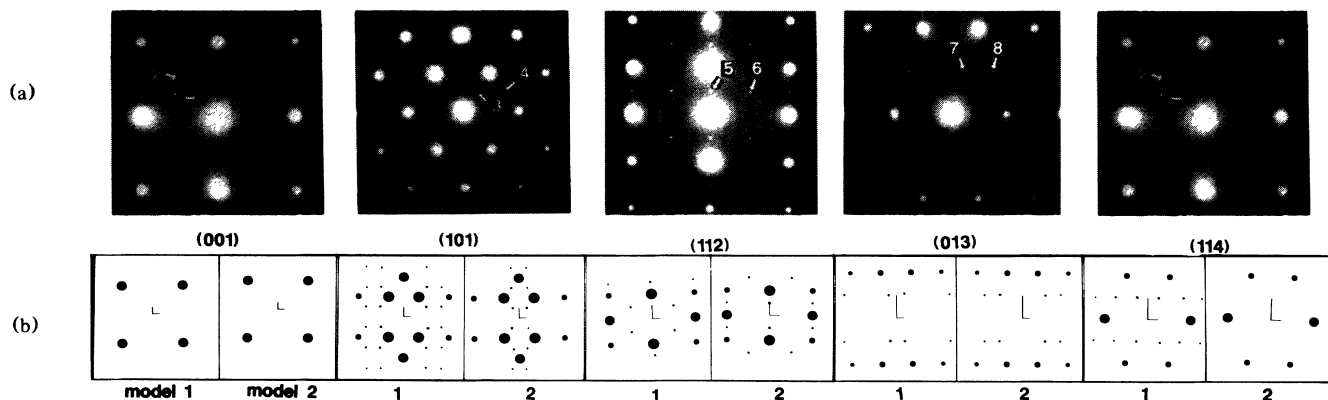


FIG. 4. (a) Diffraction patterns obtained from a planar-view sample. The arrows refer to extra reflections described in Table I. (b) Simulated diffraction patterns for models 1 and 2. Note that in the simulations, the reflections due to double diffraction in the SiGe lattice are not included, i.e., the (200)-type spots are not present for the (101) and (013) zone axes.

directly shown to be associated with superlattice reflections.

Two possible structures have been proposed⁶ that are consistent with the diffraction pattern reported by Ourmazd and Bean. These are shown in Fig. 5. Ourmazd and Bean only considered the model shown in Fig. 5(a) (model 1), but Littlewood⁷ pointed out that the model shown in Fig. 5(b) (model 2) could also explain the observed diffraction pattern. Since we obtained diffraction patterns along several zone axes, and since the superlattice reflections are strong, it is now possible to determine the exact structure of the ordered phase. Figure 4(b) shows simulated diffraction patterns obtained using models 1 and 2, and Table I gives the calculated intensities for both models. Note that all four variants have been superimposed to obtain the simulated diffractions, so that they can be directly compared with the experimental diffraction patterns. All of the superlattice reflections [except the one along (100)], as well as their intensities, are consistent with model 2 only. This is true even when one considers the possible complication of the diffraction

pattern due to the presence of twins; thin twins along $\langle 111 \rangle$ generate elongated rods in reciprocal space. When intersecting a plane different from the habit plane of the twins, these rods give rise to apparent extra spots. For example, thin twins in SiGe can result in extra diffraction spots at $\frac{1}{2}\{113\}$.¹² The same twin would also generate extra spots, but of lower intensity, at $\frac{1}{2}\{313\}$, thus lowering the apparent ratio of intensities between the $\frac{1}{2}\{313\}$ and $\frac{1}{2}\{113\}$ spots. Still, we clearly observe that the $\frac{1}{2}\{313\}$ spots are brighter than the $\frac{1}{2}\{113\}$ spots.

The weak extra spots along (100) can be explained either by the presence of domain boundaries (see Fig. 3), where the periodicity along (100) would indeed be broken, or by "stacking faults," where two units such as the ones shown in Fig. 5(b) would be next to each other, instead of alternating with units where Ge atoms replace Si atoms.

Several theoretical studies have been done to explain the ordering in SiGe. Littlewood⁷ and Martins and Zunger⁸ discarded model 2 because, in contrast to model

TABLE I. Lattice reflections corresponding to the superlattice reflections marked in Fig. 4, calculated structure factor associated with each superlattice reflection for models 1 and 2, and observed intensities.

No. in Fig. 4	Corresponding lattice reflection	$ F^2 /16^2(F_{Si} - F_{Ge})^2$ (using unit cell described in Fig. 5)		Experimental observation
		Model 1	Model 2	
1	{100}	0	0	Very weak
2	{200}	0	0	Very weak
3	$\frac{1}{2}\{111\}$	$2 - \sqrt{2}$	$2 + \sqrt{2}$	Stronger than 4
4	$\frac{1}{2}\{131\}$	$2 + \sqrt{2}$	$2 - \sqrt{2}$	Weak
5	$\frac{1}{2}\{111\}$	$2 - \sqrt{2}$	$2 + \sqrt{2}$	Stronger than 6
6	$\frac{1}{2}\{113\}$	$2 + \sqrt{2}$	$2 - \sqrt{2}$	Weak
7	$\frac{1}{2}\{131\}$	$2 + \sqrt{2}$	$2 - \sqrt{2}$	Weak
8	$\frac{1}{2}\{331\}$	$2 - \sqrt{2}$	$2 + \sqrt{2}$	Stronger than 7
9	$\frac{1}{2}\{113\}$	$2 + \sqrt{2}$	$2 - \sqrt{2}$	Weak

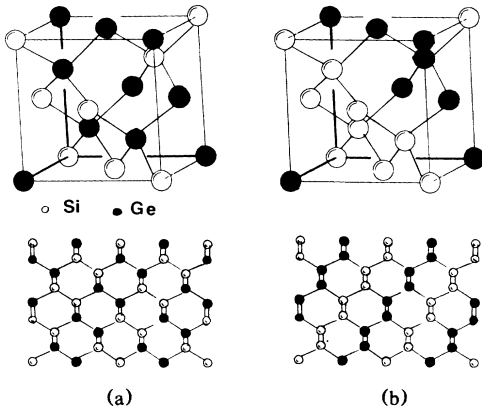


FIG. 5. Models consistent with previous work. Top, one eighth of the ordered unit cell. To obtain the complete unit cell, one has to alternate, in the x , y , and z directions, unit cells similar to the ones shown here, with unit cells where the Ge atoms replace Si atoms, and vice versa. Bottom, (101) cuts through one unit cell.

1, it is strained microscopically. Ciraci and Batra⁹ included model 2 in their calculations, but only for strained layers, and concluded that it had a higher energy than model 1. Both Ciraci and Batra and Littlewood concluded that strain was necessary to observe ordering. Martins and Zunger concluded that strain would indeed help the formation of an ordered phase by making it more stable, but also showed (for model 1 only) that the ordered phase was metastable or possibly “weakly” stable even without strain. The fact that model 2 is found to be the structure of the ordered phase is not necessarily in contradiction with these theoretical calculations since all the calculations either did not consider model 2 or assumed that the layers were strained. We note that Martins and Zunger calculated that the Si-Ge bond is weaker than either the Si-Si or the Ge-Ge bond. They used this calculation to explain why model 1 (with 75% Si-Ge bonds) should be preferred over a zinc-blende type of ordering (with 100% Si-Ge bonds). Model 2 has only 25% Si-Ge bonds and thus has an even lower chemical energy than model 1. Martins and Zunger pointed out that model 2 is microscopically strained (unlike model 1), so that a finite mechanical energy would have to be added to the total energy. They calculated this energy to be small in SiGe alloys, so that it is conceivable that the chemical energy term would play the determining role. It is also important to note that, since the ordering occurs along the four (111) directions, the total aggregate strain is zero.

The presence of ordering in thick, relaxed (indeed, bulklike) layers is surprising since it is generally accepted that bulk SiGe alloys do not order. It is likely that some residual strain remains. But, as demonstrated by the lattice-parameter measurement, this remaining strain is orders of magnitude lower than the strain present in the strained multilayer studied by Ourmazd and Bean,

as well as the strain assumed in the theoretical calculations. It is possible that the growth mode plays a considerable role in the formation of a weakly stable phase. It is known from previous studies¹³ that Si and Ge are not deposited randomly in the apparatus used to grow the present sample. Indeed, they tend to form a very thin “superlattice” in the direction of the growth (100) because of the rotation of the sample and of the relative position of the Si and Ge beams. It is conceivable that this artificial ordering, as well as the surface reconstruction mentioned by Ciraci and Batra lowers the nucleation barrier enough to form a weakly stable ordered phase. The growth temperature also plays a considerable role in this ordering. Indeed, in Ref. 10, where no ordering was observed, the samples were grown at 580–600°C, or about 200°C higher than our samples. The systematic effect of temperature is now under investigation. Boron is clearly not a factor in the formation of this new stable phase since when the simpler sample, with no boron and no underlying structure, was studied, the same ordering was found to occur. Another surprising aspect of the ordering phenomenon in this system is that it occurs along all four possible $\langle 111 \rangle$ variants. In most other systems only two variants have been observed, although for the SiGe case, studies done so far did not try to determine whether two or four variants were present.

We would like to thank Dr. T.-S. Kuan for extensive discussions and U. Gensser and B. Ek for their technical assistance.

¹T. S. Kuan, T. E. Kuech, W. I. Wang, and E. L. Wilkie, *Phys. Rev. Lett.* **54**, 201 (1985).

²A. Ourmazd and J. C. Bean, *Phys. Rev. Lett.* **55**, 765 (1985).

³D. J. Lockwood, K. Rajan, E. W. Fenton, J.-M. Baribeau, and M. W. Denhoff, *Solid State Commun.* **61**, 465 (1987).

⁴T. S. Kuan, in *Encyclopedia of Physical Science and Technology*, edited by K. A. Meyers (Academic, New York, 1989), p. 521.

⁵T. Suzuki and A. Gomyo, *J. Appl. Phys.* **27**, 2098 (1988).

⁶M. Hansen, *Constitution of Binary Alloys* (McGraw-Hill, New York, 1958), 2nd ed., p. 774.

⁷P. B. Littlewood, *Phys. Rev. B* **34**, 1363 (1986).

⁸J. L. Martins and A. Zunger, *Phys. Rev. Lett.* **56**, 1400 (1986).

⁹S. Ciraci and I. P. Batra, *Phys. Rev. B* **38**, 1835 (1988).

¹⁰T. S. Kuan, S. S. Iyer, and E. M. Yeo, in *Proceedings of the Forty-Seventh Annual Meeting of the Electron Microscopy Society of America*, edited by G. W. Bailey (San Francisco, San Francisco, 1989), p. 580.

¹¹T. S. Kuan (private communication).

¹²S. S. Iyer and F. K. LeGoues, *J. Appl. Phys.* **65**, 4693 (1989).

¹³U. Gensser, V. P. Kesan, T. J. Bralot, and S. S. Iyer, in *Proceedings of the Tenth Molecular-Beam Epitaxy Workshop*, Raleigh, North Carolina [J. Vac. Sci. Technol. (to be published)].

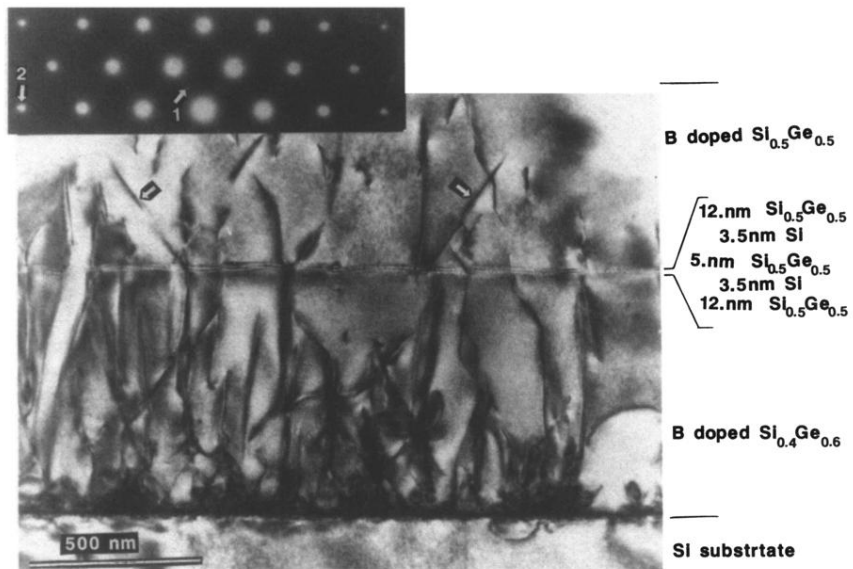


FIG. 1. Cross-sectional view and diffraction pattern of the samples. The arrows on the image show twins. In the diffraction pattern, the arrow marked 1 shows the extra spot due to ordering. The arrow marked 2 shows the splitting of the high-order spots due to the mismatch between substrate and layer.

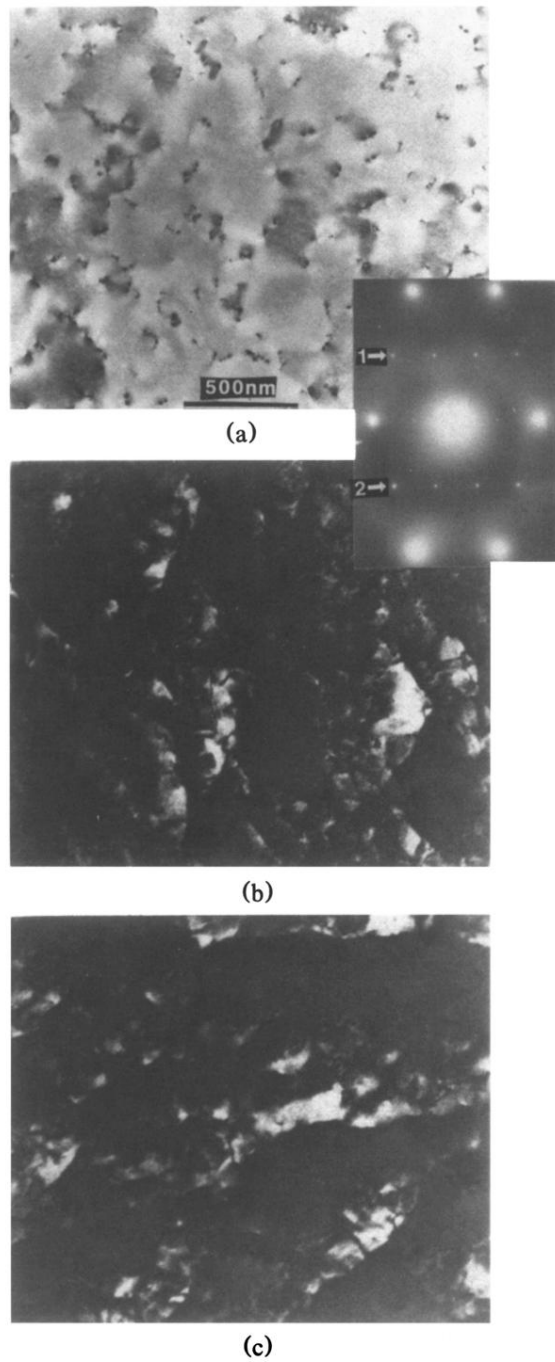


FIG. 2. (a) Bright field and diffraction pattern corresponding to the dark fields shown in (b) and (c). The zone axis is (013). (b) Dark field obtained using spot 1 on diffraction pattern. (c) Dark field obtained using spot 2 on diffraction pattern.

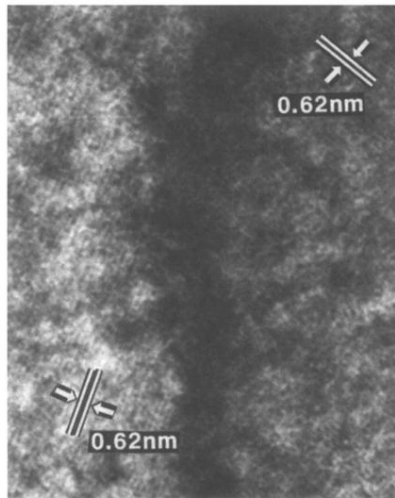


FIG. 3. High resolution of a domain boundary between two ordered zones with different orientations.

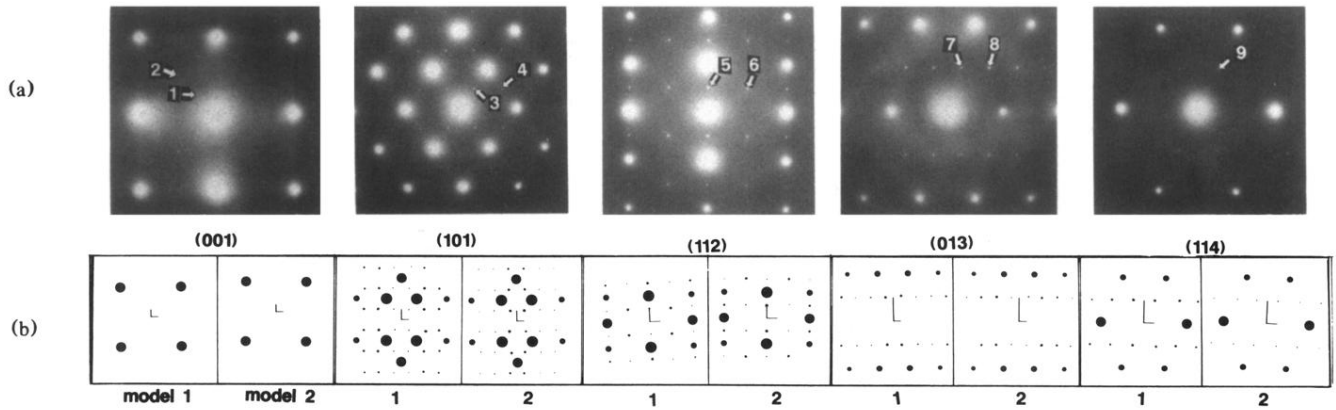


FIG. 4. (a) Diffraction patterns obtained from a planar-view sample. The arrows refer to extra reflections described in Table I. (b) Simulated diffraction patterns for models 1 and 2. Note that in the simulations, the reflections due to double diffraction in the SiGe lattice are not included, i.e., the (200)-type spots are not present for the (101) and (013) zone axes.